

Original Article

Open Access



# Computational evaluation of mitral valve repair with MitraClip

Brandon Prescott<sup>1</sup>, Chad J. Abunassar<sup>2</sup>, Konstantinos P. Baxevanakis<sup>1</sup>, Ligu Zhao<sup>1,3</sup>

<sup>1</sup>Wolfson School of Mechanical, Electrical and Manufacturing Engineering, Loughborough University, Epinal Way, Loughborough LE11 3TU, UK.

<sup>2</sup>Abbott Vascular, 3200 Lakeside Drive, Santa Clara, CA 95054, USA.

<sup>3</sup>School of Mechanical and Equipment Engineering, Hebei University of Engineering, Handan 056038, China.

**Correspondence to:** Prof. Ligu Zhao, Wolfson School of Mechanical, Electrical and Manufacturing Engineering, Loughborough University, Epinal Way, Loughborough, LE11 3TU, UK. E-mail: L.Zhao@Lboro.ac.uk

**How to cite this article:** Prescott B, Abunassar CJ, Baxevanakis KP, Zhao L. Computational evaluation of mitral valve repair with MitraClip. *Vessel Plus* 2019;3:13. <http://dx.doi.org/10.20517/2574-1209.2018.70>

**Received:** 7 Nov 2018 **First Decision:** 14 Jan 2019 **Revised:** 12 Feb 2019 **Accepted:** 4 Mar 2019 **Published:** 19 Apr 2019

**Science Editor:** Alexander D. Verin **Copy Editor:** Cai-Hong Wang **Production Editor:** Huan-Liang Wu

## Abstract

**Aim:** This paper aims to evaluate the effectiveness of MitraClip implantation as a solution to severe mitral regurgitation (MR) in the case of posterior leaflet prolapse due to hypertrophic obstructive cardiomyopathy and chordae rupture.

**Methods:** NX CAD software was used to create a surface geometric model for the mitral valve (MV). A hyperelastic material model, calibrated against experimental results, was used to describe stress-strain responses of the MV leaflets, and a spring element approach was used to describe chordae response. Abaqus CAE was employed to create a finite element model for diseased MV suffering from MR. The effectiveness of MitraClip implantation on valve function was investigated by simulating the deformation of diseased valve, with and without MitraClip repair, during peak systole and diastole. Leaflet deformation and stress distributions were used to assess the effectiveness of the procedure.

**Results:** Overall, significant improvement was achieved for the diseased valve after MitraClip implantation. Prior to the introduction of the clip, the diseased valve was subjected to posterior leaflet prolapse which would induce a jet of MR. Once the MitraClip was included in the simulation, the valve leaflets were able to close and seal off, almost entirely at peak systolic condition without a significant impact on the stress distribution of the valve leaflets.

**Conclusion:** The results in this study provide further evidence to support MitraClip repair as a viable treatment for high-risk patients suffering from severe MR, and also highlight the need for further research into such an advanced, minimally invasive surgery technique.



© The Author(s) 2019. **Open Access** This article is licensed under a Creative Commons Attribution 4.0 International License (<https://creativecommons.org/licenses/by/4.0/>), which permits unrestricted use, sharing, adaptation, distribution and reproduction in any medium or format, for any purpose, even commercially, as long as you give appropriate credit to the original author(s) and the source, provide a link to the Creative Commons license, and indicate if changes were made.



**Keywords:** Finite element, mitral valve, MitraClip, mitral regurgitation, hypertrophic obstructive cardiomyopathy, hyperelastic model

## INTRODUCTION

The mitral valve (MV) is a complex apparatus, mainly consisting of mitral annulus, anterior and posterior leaflets, chordae tendineae and two sets of papillary muscles. The MV is situated between the left atrium and the left ventricle, which, under regular healthy conditions, ensures that blood can only flow in one direction. Therefore, there are two key stages to understand the function of the MV. Firstly, the valve allows blood to flow from the left atrium to the left ventricle during diastolic ventricular filling, and secondly, the valve prevents backflow of blood into the left atrium during systolic ventricular ejection<sup>[1]</sup>. If the valve is diseased, it cannot ensure a unidirectional flow of blood into the left ventricle, causing the back flow of blood into the left atrium during systole, a condition known as mitral regurgitation (MR). There are multiple notable causes of MR, but this study will focus on posterior leaflet prolapse and ruptured chordae tendineae in the context of hypertrophic obstructive cardiomyopathy (HOCM)<sup>[2]</sup>.

A population-based study into the burden of valvular heart diseases highlighted that MR is the most common heart disease in the western population, and the prevalence of the disease rose strikingly with advancing age<sup>[3]</sup>. For this reason, there is a lot of interest in developing safer and more repeatable procedures for the treatment of MR. More specifically, there is a push to develop procedures which are less invasive than conventional open-chest surgery, as a large number of patients (as many as 49%) with MR in need of repair or replacement are considered at high risk for surgical intervention<sup>[4]</sup>. Reasons for this high risk association can be due to the patients' age and other comorbidities (the presence of additional diseases co-occurring with the primary disease) and the result is that the patients simply do not qualify for conventional open-chest surgery<sup>[5]</sup>.

The MitraClip system is a minimally invasive procedure to treat MR in the case where a patient isn't eligible for open-chest surgery. Unlike conventional surgery, the MitraClip procedure does not require opening of the chest. Instead, clinicians access the MV with a catheter that is guided through a vein in the patient's leg to reach the heart<sup>[6]</sup>. There are also a lot of cases which suggest that the MitraClip system is in fact an effective approach for the treatment of severe MR in practice. The initial Egyptian experience study into percutaneous mitral repair with MitraClip system demonstrated that, out of five patients, procedural success was achieved in all patients (100%). There was no procedural mortality after 30 days. In addition to the reduction in MR severity, the clinical status improved in 4 patients (80%) at discharge<sup>[7]</sup>. Furthermore, the initial French experience provided additional evidence to support the positive effects of MitraClip implantation. The study was based on the treatment of 62 patients (72.7 ± 11.4 years; 71.7% men; New York Heart Association (NYHA) class III or IV; MR ≥ grade 3) and assessed their conditions pre and post treatment. The study concluded that the in-hospital mortality rate was 3.2%, survival rate at 6 month follow up was 83.1%, with 90.9% of patients in NYHA class I or II and residual MR ≤ grade 2 in 80% of cases<sup>[8]</sup>. So, despite being an initial learning phase, the results should be seen as promising for the patients who are ineligible for open-chest surgery. That being said, there is a clear indication for further improvement of the MitraClip system, particularly the use of simulation work and clinical trials to further understand the MV and its interaction with the MitraClip.

Therefore, the aim of this paper is to investigate the effects of MitraClip implantation on regurgitant MV function, in terms of the valve's ability to close entirely during systole as well as stress distribution across the valve leaflets at peak systole and diastole, in a finite element (FE) environment.

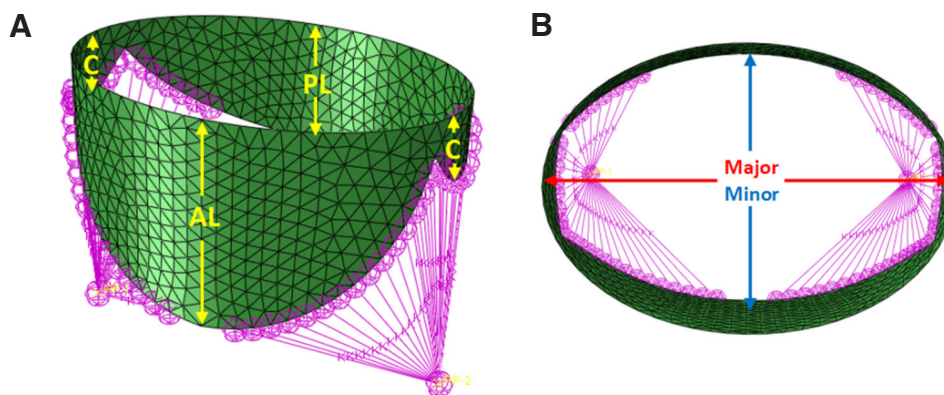


**Figure 1.** Initial configuration for diseased valve without MitraClip: (A) isometric view; (B) aerial view

## METHODS

### Description of mitral valve model

Simulations were carried out by Abaqus explicit solver<sup>[9]</sup>. The step time was 1 s for the systolic step in all simulations. The stable time increment was of the order  $10^{-6}$  s throughout the analysis. The MV geometry was created using surface modelling tools available in NX<sup>[10]</sup> and dimensions were based on an anatomic study into intact and excised valves<sup>[11]</sup>. Notably, the anterior leaflet, posterior leaflet and commissures have a height of 18 mm, 11 mm and 6 mm, respectively. The annulus was approximated to an elliptical profile with a major axis of 34 mm and a minor axis of 24 mm [Figure 1]. The main steps to create the geometric model were extruding an ellipse to form a solid body, then creating planar sketches for the anterior and posterior leaflet profiles, and finally projecting these sketches around the solid body. The result was a planar surface contained within a 3D modelling space which could then be imported into Abaqus to complete the pre-processing stages.

The geometry was discretised into 1,023 S3 shell elements (3-node triangular general-purpose shell, finite membrane strains) and a thickness of 1 mm was assigned to each element (the thickness was assumed uniform across the tissue). A series of spring elements were attached to the free edge of the leaflets to represent the chordae tendineae. A stiffness of 1.6 N/mm was assigned to each spring<sup>[12]</sup>. Two reference points were used to account for the papillary muscles.

The simulations were carried out for two separate models. The first configuration was the diseased valve without a clip, aiming to understand how the MV is failing to operate [Figure 1].

The second configuration employed a reconstructed geometry, where the central regions of the anterior and posterior leaflets were clamped together to represent the MitraClip implanted [Figure 2].

### Interaction, loading and boundary conditions

The motion and pressures in which the MV apparatus experiences during systole and diastole are completely governed by its interaction with blood flow as it passes from the left atrium to the left ventricle. Since blood will not be explicitly modelled within the FE simulation, appropriate boundary conditions and loading will need to be applied to the valve to capture this interaction.

In both simulations, a linearly increasing ventricular pressure from 0 to 120 mmHg (0.016 MPa) was applied to the outer surfaces of the valve to represent systolic peak during the first step. In the second step, a linearly increasing pressure from 0 to 5 mmHg (0.0007 MPa) was applied to the inner surfaces of the valve to represent diastole. The annulus and papillary muscles were fully constrained, and the effect of papillary

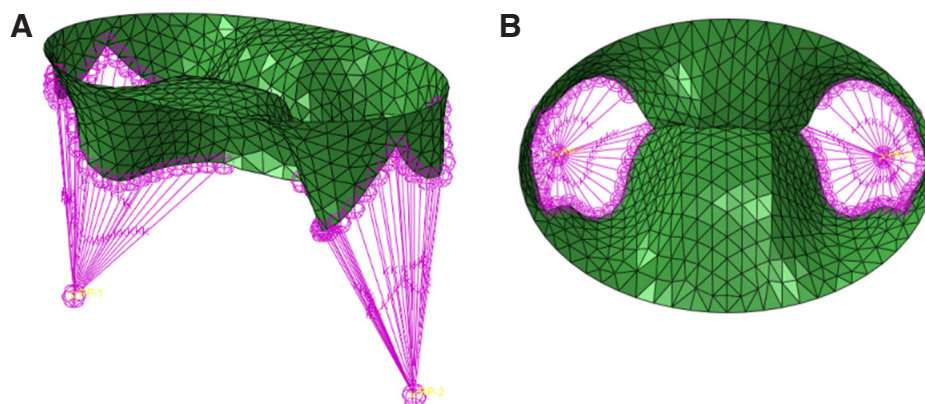


**Figure 2.** Initial configuration for diseased valve with MitraClip: (A) isometric view; (B) aerial view

muscle displacement and annular motion on the stress pattern was shown negligible at systolic peak<sup>[13]</sup>. For the second simulation, the central-region nodes were also fully constrained to represent the MitraClip. In this study, MitraClip was not modelled explicitly in the FE simulations. Instead, full constraints have been used to define the MitraClip's interaction with the leaflets. The amount of interaction between the anterior and posterior leaflets was decided based on the dimension of the MitraClip, taken from Abbott's product specification<sup>[14]</sup>. Specifically, a total of 114 elements in the central region of the leaflets (78 elements for anterior and 36 elements for posterior) were fully constrained to define the interaction between the anterior and posterior leaflets as a result of the clip.

A surface to surface contact condition was defined between all the inner surfaces of the MV. For the normal behaviour, hard contact was used to model the overclosure response, and separation was allowed after contact. For the tangential behaviour, a penalty friction formulation was used, and the value of friction coefficient assigned was taken as 0.05. Directionality of friction was assumed to be isotropic. This interaction has been previously justified, as it characterises the contact between soft and wet surfaces, such as hydrogels, whose surface behaviour may be considered a good approximation for the leaflets in the absence of further experimental data. The use of the penalty contact algorithm (assumes surfaces start to interact just before they actually touch each other) is also justified as *in-vivo* leaflets do actually start to interact before coapting, since just before actual contact a blood film is trapped between them and then moved away by the leaflets<sup>[15]</sup>.

### Material model

A 5th order hyperelastic reduced polynomial model (available in Abaqus CAE) was adopted to describe the mechanical behaviour of the MV tissue. This model assumes that the deformation of the material can be described by a strain energy density formulation, from which the stress-strain relationship can be derived. The strain energy density equation is defined as<sup>[16]</sup>:

$$U = \sum_{i=1}^N C_{i0} (\bar{I}_1 - 3)^i + \sum_{i=1}^N \frac{1}{D_i} (J^{el} - 1)^{2i} \quad (1)$$

where  $U$  is the strain energy per unit of reference volume,  $N$  is a material parameter,  $C_{i0}$  and  $D_i$  are temperature-dependent material parameters. Here,  $\bar{I}_1$  is the first deviatoric strain invariant defined as:

$$\bar{I}_1 = \bar{\lambda}_1^2 + \bar{\lambda}_2^2 + \bar{\lambda}_3^2 \quad (2)$$

where the deviatoric stretches  $\bar{\lambda}_i = J^{-\frac{1}{3}} \lambda_i$ ,  $J$  is the total volume ratio,  $J^{el}$  is the elastic volume ratio and  $\lambda_i$  are the principal stretches.

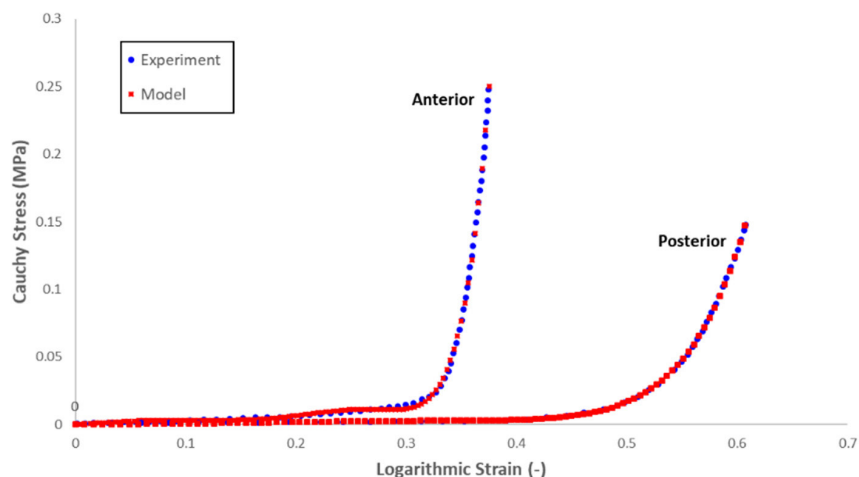


**Figure 3.** Radial stress-strain response of human hypertrophic obstructive cardiomyopathy anterior and posterior leaflet samples, experimental data vs. model simulation

**Table 1.** Reduced polynomial material parameters used to define the mechanical behaviour of the mitral valve tissue

Leaflet	C <sub>10</sub>	C <sub>20</sub>	C <sub>30</sub>	C <sub>40</sub>	C <sub>50</sub>	D <sub>1</sub>	D <sub>2</sub>	D <sub>3</sub>	D <sub>4</sub>	D <sub>5</sub>
Anterior	0.00964	-0.106	0.788	-2.364	2.514	0.001	0	0	0	0
Posterior	0.00110	0.00152	-0.00389	0.00222	0.00079	0.001	0	0	0	0

For the anterior leaflet, the model parameters were obtained by fitting the constitutive equation to experimental radial stress-strain data of HOCM anterior valve tissue provided in the literature<sup>[17]</sup>. It should be noted that the anterior and posterior leaflets exhibit different mechanical behaviour, with the posterior leaflet having higher extensibility (i.e., lower stiffness). Due to a lack of stress-strain data for the HOCM posterior leaflet, a shift, based on the difference measured for healthy anterior and posterior leaflets<sup>[17]</sup>, has been applied to the stress-strain data for HOCM anterior leaflet in order to capture the increased extensibility of a posterior leaflet. The shifted stress-strain data were then used to calibrate the model parameters for the HOCM posterior leaflet. The resulting curve fit and model parameters can be seen in [Figure 3](#) and [Table 1](#), respectively, and were obtained by conducting single-element simulation using the described material model. The compressibility (*D*) parameters were fixed based on the assumption of MV tissue being “nearly incompressible”<sup>[18]</sup>, whilst the *C* values were refined iteratively to obtain the closest fit. A density of 10.4 g/cm<sup>3</sup> was assigned to all MV tissue. This value is ten times higher than the actual value to account for the inertial effects of blood flow<sup>[13]</sup>.

As aforementioned, the mechanical behaviour of the chordae tendineae was described using a simplified spring stiffness approach. The value of 1.6 N/mm was estimated according to chordae properties given in the literature<sup>[12]</sup>. The use of built-in SPRINGA elements from the Abaqus library is ideal for simulating the response of the chordae tendineae, as this element is able to transmit axial load through a line of action and this line of action is able to rotate when subjected to large-displacement analysis<sup>[19]</sup>, which is characteristic of the simulations within this study.

## RESULTS

Continuum mechanics can be used to describe the deformation of structures through the use of a nine-component stress tensor. However, individually, these values can be difficult to interpret and use in a practical sense. Therefore, more informative stress values can be obtained through the use of mathematical operations, derived from the original nine-component tensor. In this study, the results were provided with

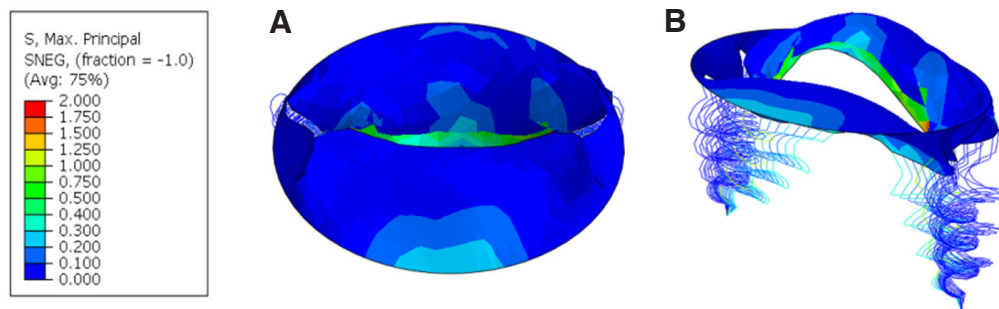


**Figure 4.** Maximum principal stress (MPa) contour plot for mitral valve at peak systole without MitraClip: (A) aerial view; (B) isometric view

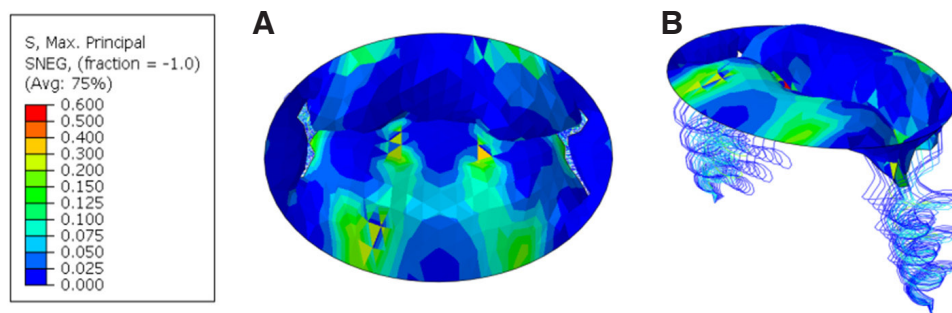


**Figure 5.** Maximum principal stress (MPa) contour plot for mitral valve at peak systole with MitraClip: (A) aerial view; (B) isometric view

respect to the maximum principal stresses in the leaflets. The principal stresses indicate the minimum and maximum normal stresses an element will undergo for the given external loading conditions.

### Systole

Figures 4 and 5 show the simulation results for the diseased valve operating at peak systole, without and with the MitraClip, respectively. The deformation scale factor is set to 1 for true representation.

It can be seen from [Figure 4](#) that the posterior leaflet has prolapsed due to a combination of the increased extensibility of HOCM leaflets and the ruptured chordae presented in the model. The area created by this prolapse would allow for a regurgitant jet to pass blood back into the left atrium and subsequently cause MR. In terms of the stress distribution, it generally falls in the range of 50-300 kPa across most of the valve's surface. However, there is a large stress concentration of approximately 2.0 MPa in the region where the prolapsed leaflet is attached to the chordae. This can be expected due to the unnaturally large amount of deformation experienced by the posterior leaflet during these prolapsed conditions. That being said, the key finding highlighted by [Figure 4](#) is the displacement of the posterior leaflet, and how its position at peak systole is preventing complete closure of the MV leaflets.

From [Figure 5](#), it can be seen that the introduction of the MitraClip has affected the MV function at peak systole. The central region of the leaflets, fixed together as a result of clip implantation, has solved the previous issue of prolapse. From the aerial view, it can also be seen that the valve has almost completely sealed off any gaps which were present before. The order of magnitude of stress has not been affected significantly by the introduction of the MitraClip across the majority of the surfaces.

In terms of specific values, the stress distribution generally falls in the range of 50-300 kPa across the majority of the valve's surface, similar to the simulation without MitraClip [[Figure 4](#)]. However, the introduction of the clip has significantly reduced the peak stress experienced by the valve to a value of

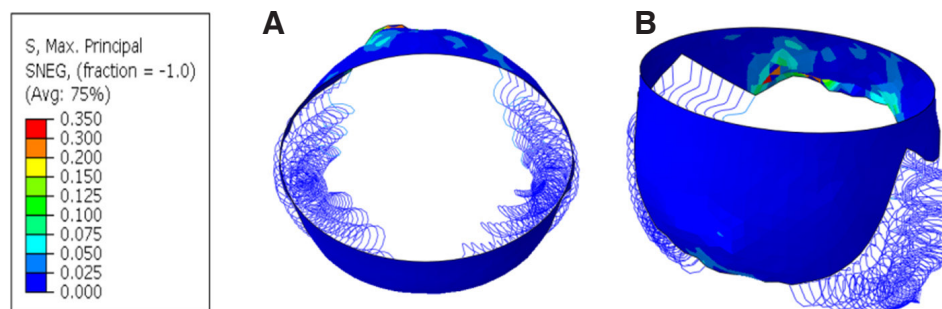


**Figure 6.** Maximum principal stress (MPa) contour plot for mitral valve at peak diastole without MitraClip: (A) aerial view; (B) isometric view

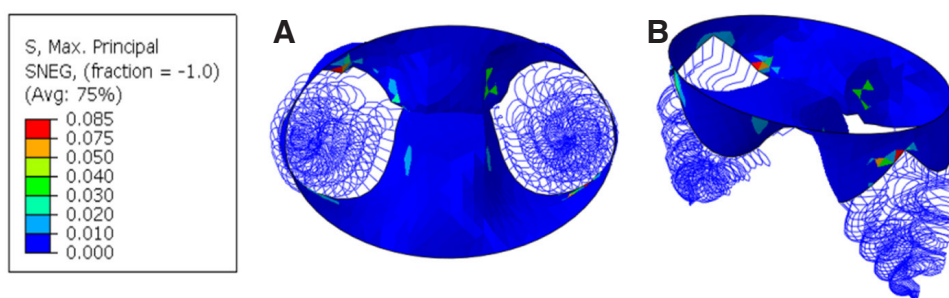


**Figure 7.** Maximum principal stress (MPa) contour plot for mitral valve at peak diastole with MitraClip: (A) aerial view; (B) isometric view

approximately 600 kPa (compared to 2.0 MPa for the simulation without MitraClip; [Figure 4](#)). This is because the fixed central region of the leaflets eliminated the stress caused by posterior leaflet prolapse. [Figure 5](#) highlights that the MitraClip has not only improved the MV function in terms of its ability to coapt successfully, but also alleviated the local increase in stress due to prolapse.

### Diastole

[Figures 6 and 7](#) show the valve operating during diastole, without and with the MitraClip, respectively. The MV is subjected to a reduced level of stress during diastole due to the lower atrial pressure applied and the lack of surface interaction between the leaflets.

In [Figure 6](#), the region where the chordae are ruptured leads to an increase in stress relative to the rest of the valve. This follows a similar pattern to the stress concentration presented in [Figure 4](#); however, the order of magnitude is much lower. The stress distribution across the leaflets generally falls in the range of 0 to 75 kPa, and peak stress occurs in the regions on the posterior leaflet where the chordae was attached, with a magnitude of approximately 350 kPa. The increased extensibility of the HOCM leaflets and ruptured chordae has also caused the posterior leaflet to displace further in the ventricular direction than what would be seen under healthy conditions.

[Figure 7](#) highlights the “double orifice area” induced by the clip during diastole. This is a key feature that arises as a result of the anterior and posterior leaflets being clamped together through the use of a clip. As the central region of the valve leaflets are fixed together, a small gap is created on either side of the clip during diastolic ventricular filling. The double orifice area is a crucial characteristic after edge-to-edge repair of the MV, as it acts as passageway for blood to flow through during diastole but allows for the leaflets to completely close up and seal off backflow of blood during systolic ventricular ejection<sup>[20]</sup>.

Even with the presence of a double orifice area, the majority of the valve is still subjected to a relatively low level of stress (less than 30 kPa), with a few small areas of stress concentration due to the attachment of the

chordae. Again, the peak stress has been reduced by the introduction of the MitraClip to a value of 85 kPa during diastole.

## DISCUSSION

Previous clinical trials have reported the successful use of the MitraClip system as a solution for severe MR in the context of HOCM. A study of six patients suffering from the disease concluded that percutaneous mitral repair using the MitraClip is feasible and may be performed safely in HOCM, and this technique can be effective in reducing MR and improving symptoms<sup>[21]</sup>. This is supported by clinical trial which reported that patients experienced a reduction in MR and a reduction in the left ventricular outflow tract (LVOT) gradient from a mean of  $75.8 \pm 39.7$  to  $11.0 \pm 5.6$  mmHg<sup>[22]</sup>. Nearly all patients demonstrated improvements in symptoms by either new NYHA class designations or improved exercise tolerance<sup>[22]</sup>.

The results of our FE simulations provided further evidence to support that MitraClip implantation is a viable approach for solving MR in the case of posterior leaflet prolapse due to HOCM leaflet extensibility and chordae rupture. The introduction of the clip has prevented the leaflet from prolapsing and aided in almost complete closure of the valve during peak systole. The general order of magnitude of stress across the leaflets has not been affected significantly by the clip during systole and diastole. In fact, in the previously prolapsed region where the chordae are present, the MitraClip has alleviated stress significantly.

There have been a number of previous studies into FE modelling of the MV apparatus with a focus on topics such as nonlinear tissue response, annulus dilation and relative papillary muscle motion. However, the literature is limited regarding simulations of the MitraClip system in an FE environment, and also addressing the diastolic stage. The novelty of the current study lies with the concise side-by-side comparison of the same diseased valve, operating under the same loading conditions, with and without the MitraClip, respectively. The performance of the valve has been assessed under both peak systolic and peak diastolic conditions, and a quantifiable improvement in MV function has been established after introduction of the clip. Therefore, the results should aid in a better understanding of the implications that the MitraClip system has on both the stress distribution and deformation of the MV leaflets. This information may aid in further development of the MitraClip and should encourage further research into advanced, minimally invasive treatments for severe MR in high risk patients.

Further work is also needed to refine the FE method employed in the current study to more accurately capture the impact of HOCM and produce more comprehensive results in the future. Notably, the effects of annulus dilation and relative papillary motion will have to be accounted for to produce a less conservative model. Furthermore, a deeper analysis into simulating systolic anterior motion would be beneficial due to the risk of LVOT obstruction and MR, which is associated with a 20% risk of sudden death<sup>[23]</sup>. That being said, the current study has provided a solid ground to extend to these related areas. In addition, a fluid-structure interaction (FSI) model would be more helpful for analysing MitraClip behaviour during diastolic stage. Some previous computational studies have employed FSI approach in modelling and understanding the function of mitral valve<sup>[24,25]</sup>, but not in the context of MitraClip repair. To run an appropriate FSI analysis for mitral valve repaired with MitraClip, it will require tremendous additional efforts and times, and seems beyond the scope of current study. Nevertheless, the research group are currently undertaking such analyses and the results will be reported in future.

## DECLARATIONS

### Authors' contributions

Contributed to the research and the preparation of the manuscript: Prescott B, Abunassar CJ, Baxevanakis KP, Zhao L

Carried out the work, processed the results and drafted the manuscript: Prescott B

Supervised the technical work and also contributed to discussions, writing and editing of the manuscript: Abunassar CJ, Baxevanakis KP, Zhao L

### Availability of data and materials

Further data and materials are available upon request to Professor Liguó Zhao at Loughborough University (email: L.Zhao@Lboro.ac.uk).

### Financial support and sponsorship

None.

### Conflicts of interest

The authors declared that there are no conflicts of interest.

### Ethical approval and consent to participate

Not applicable.

### Consent for publication

Not applicable.

### Copyright

© The Author(s) 2019.

## REFERENCES

1. Sturla F, Redaelli A, Puppini G, Onorati F, Faggian G, et al. Functional and biomechanical effects of the Edge-to-Edge repair in the setting of Mitral regurgitation: consolidated knowledge and novel tools to gain insight into its percutaneous implementation. *Cardiovasc Eng Technol* 2015;6:117-40.
2. Staff MC. MV regurgitation symptoms. Available from: <https://www.mayoclinic.org/diseases-conditions/mitral-valve-regurgitation/symptoms-causes/syc-20350178>. [Last accessed on 8 Apr 2019]
3. Nkomo VT, Gardin JM, Skelton TN, Gottdiener JS, Scott CG, et al. Burden of valvular heart diseases: a population-based study. *Lancet* 2006;368:1005-11.
4. Wan B, Rahnavardi M, Tian DH, Phan K, Munkholm-Larsen S, et al. A meta-analysis of MitraClip system versus surgery for treatment of severe mitral regurgitation. *Ann Cardiothorac Surg* 2013;2:683-92.
5. Taramasso M, Buzzatti N, La Canna G, Colombo A, Alfieri O, et al. Interventional vs. surgical mitral valve therapy. Which technique for which patient? *Herz* 2013;38:460-6.
6. Abbott. Can the MitraClip procedure help me? Available from: [http://mitraclip.com/can\\_the\\_mitraclip\\_procedure\\_help\\_me](http://mitraclip.com/can_the_mitraclip_procedure_help_me). [Last accessed on 8 Apr 2019]
7. Khamis H, Abdelaziz A, Ramzy A. Percutaneous mitral repair with MitraClip system; safety and efficacy; initial Egyptian experience. *Egypt Hear J* 2014;66:11-6.
8. Armoiry X, Brochet E, Lefevre T, Guerin P, Dumonteil N, et al. Initial French experience of percutaneous mitral valve repair with the MitraClip: a multicentre national registry. *Arch Cardiovasc Dis* 2013;106:287-94.
9. Simulia. Abaqus/CAE User's Guide. Available from: [http://130.149.89.49:2080/v6.14/pdf\\_books/CAE.pdf](http://130.149.89.49:2080/v6.14/pdf_books/CAE.pdf). [Last accessed on 8 Apr 2019]
10. Siemens. NX 11 Help. Available from: [https://docs.plm.automation.siemens.com/tdoc/nx/11/nx\\_help/#uid:index](https://docs.plm.automation.siemens.com/tdoc/nx/11/nx_help/#uid:index). [Last accessed on 8 Apr 2019]
11. Kunzelman KS, Cochran RP, Verrier ED, Eberhart RC. Anatomic basis for Mitral valve modelling. *J Heart Valve Dis* 1994;3:491-6.
12. Votta E, Maisano F, Soncini M, Redaelli A, Montevocchi FM, et al. 3-D computational analysis of the stress distribution on the leaflets after edge-to-edge repair of mitral regurgitation. *J Heart Valve Dis* 2002;11:810-22.
13. Cochran R, Chuong C, Ring W, Verrier E, Eberhart R, et al. Finite element analysis of the mitral valve. *J Hear Valve Dis* 1993;2:326-40.
14. Abbott. MitraClip. Available from: [https://www.accessdata.fda.gov/cdrh\\_docs/pdf10/P100009c.pdf](https://www.accessdata.fda.gov/cdrh_docs/pdf10/P100009c.pdf). [Last accessed on 8 Apr 2019]
15. Votta E, Maisano F, Bolling SF, Alfieri O, Montevocchi FM, et al. The Geoform disease-specific annuloplasty system: a finite element study. *Ann Thorac Surg* 2007;84:92-101.
16. Manual AU. Hyperelastic behaviour of rubberlike materials. Available from: <http://130.149.89.49:2080/v6.11/books/usb/default.htm?startat=pt05ch21s05abm07.html>. [Last accessed on 8 Apr 2019]

17. Prot V, Skallerud B, Sommer G, Holzapfel GA. On modelling and analysis of healthy and pathological human mitral valves: two case studies. *J Mech Behav Biomed Mater* 2010;3:166-77.
18. May-Newman K, Yin FC. Biaxial mechanical behavior of excised porcine mitral valve leaflets. *Am J Physiol* 1995;269:H1319-27.
19. Simulia. Spring element library. Available from: <http://abaqus.software.polimi.it/v6.13/books/usb/default.htm?startat=pt06ch32s01ael26.html>. [Last accessed on 8 Apr 2019]
20. Sturla F, Vismara R, Jaworek M, Votta E, Romitelli P, et al. In vitro and in silico approaches to quantify the effects of the Mitraclip® system on mitral valve function. *J Biomech* 2017;50:83-92.
21. Pantazis A, Cheang MH, Mullen M, Elliott P, McKenna W, et al. Percutaneous mitral repair in hypertrophic cardiomyopathy. *Heart* 2014;100:A54-5.
22. Thomas F, Rader F, Siegel R. The use of MitraClip for symptomatic patients with hypertrophic obstructive cardiomyopathy. *Cardiology* 2017;137:58-61.
23. Ibrahim M, Rao C, Ashrafian H, Chaudhry U, Darzi A, et al. Modern management of systolic anterior motion of the mitral valve. *Eur J Cardiothoracic Surg* 2012;41:1260-70.
24. Kunzelman K, Einstein D, Cochran R. Fluid-structure interaction models of the mitral valve: function in normal and pathological states. *Philos Trans R Soc B Biol Sci* 2007;362:1393-406.
25. Lau KD, Diaz-Zuccarini V, Scambler P, Burriesci G. Fluid-structure interaction study of the edge-to-edge repair technique on the mitral valve. *J Biomech* 2011;44:2409-17.